

Blue electroluminescence from ZnO based heterojunction diodes with CdZnO active layers

L. Li, Z. Yang, J. Y. Kong, and J. L. Liu^{a)}

Department of Electrical Engineering, Quantum Structures Laboratory, University of California, Riverside, California 92521, USA

(Received 12 September 2009; accepted 13 November 2009; published online 11 December 2009)

p-ZnO/*i*-CdZnO/*n*-ZnO was grown on *n*-type Si substrates by plasma-assisted molecular-beam epitaxy. Rectifying *I*-*V* curves show typical diode characteristics. Blue electroluminescence emissions at around 459 nm were observed when the diodes were forward-biased at room temperature. The emission intensity increases with the increase of the injection current. Temperature dependent electroluminescence measurements suggest that the peak positions of blue emissions represent the band gap of the CdZnO active layer, which changes with the temperature. © 2009 American Institute of Physics. [doi:10.1063/1.3271770]

As a direct wide band gap material, ZnO attracts considerable attention for light emitting devices.¹ Reliable and highly efficient blue and green light emitting diodes (LEDs) are in high demand for daily uses. ZnO has some superior properties, such as large exciton binding energy of 60 meV. By alloying with MgO, the band gap of ZnO can be extended wider,² while it can also be adjusted from 3.3 to 1.8 eV by alloying with CdO.³⁻⁵ This makes ZnO based light sources emitting light from ultraviolet region to green band or even further. There have been several attempts to obtain visible light emissions from ZnO based heterojunction with CdZnO as active layers.^{6,7} However, other materials such as *p*-SiC (Ref. 7) and *p*-GaN (Ref. 7) were used as *p*-type layer. Our group has demonstrated stable Sb doped *p*-type ZnO grown on Si substrate⁸ and several ZnO hetero- and homojunction devices using Sb doped ZnO as *p*-type layer.⁹⁻¹¹ Dominant UV emissions have been achieved.¹¹ In this paper, we demonstrate ZnO based double heterojunction LED devices using Sb doped ZnO as *p*-layer, and inserted CdZnO as active layer. Visible blue emissions were observed and studied.

ZnO based heterojunction diode were grown by plasma-assisted molecular-beam epitaxy (MBE) on *n*-type (1–10 Ω cm) Si (100) substrate. Elemental Zn (6*N*), Cd (6*N*), Ga (6*N*), and Sb (6*N*) heated by effusion cells were used as metal sources. Oxygen (5*N*) plasma generated by a radiofrequency plasma generator was used as the oxygen source. The bottom inset of Fig. 3 shows the structure of the sample. A 30 nm thin layer of Ga-doped ZnO was first deposited on *n*-type Si(100) substrate at 450 °C, followed by the deposition of 100 nm CdZnO at 150 °C. Then the sample was *in situ* annealed at 800 °C for 5 min under vacuum. A 400 nm Sb-doped ZnO layer was then deposited at 500 °C. The sample was *in situ* annealed again at 800 °C for 20 min. Room temperature (RT) photoluminescence (PL) measurements were carried out using a homebuilt PL system, with a 325 nm He–Cd laser as excitation source and a photomultiplier tube behind the monochromator as detector. Sample was etched by diluted hydrochloride acid to different depth to investigate the PL emission from different layers. Heterojunction diodes were fabricated by standard photoli-

thography techniques. Etching was done using diluted hydrochloride acid to reach down to the substrate. Mesas with size of 800×800 μm² were formed on the sample. Metal contacts were deposited by e-beam evaporator. Au/Ni contacts with thicknesses of 200/10 nm were used on Sb-doped ZnO, and Au/Ti contacts with thicknesses of 200/10 nm were used for contacts on Si. Au/Ni contacts were subjected to rapid thermal annealing (RTA) under nitrogen ambient at 750 °C for 60 s to form ohmic contacts, while Au/Ti contacts were annealed by RTA at 500 °C for 60s. Current-voltage (*I*-*V*) characteristics were measured using Agilent 4155C semiconductor parameter analyzer. Electroluminescence (EL) measurements were carried out in the same system as PL measurement.

Figure 1 shows the secondary ion mass spectroscopy (SIMS) measurement results of the sample. Zn, O, and Sb uniformly distribute in the top 400 nm of the film, while Sb concentration dramatically decreases beyond 400 nm and Cd distributes across 100 nm below. A thin Ga-doped ZnO layer beneath CdZnO layer is also confirmed by the SIMS. However, the elemental profiles in the thin GaZnO (~30 nm) layer are not flat, which is due to the interdiffusion between the GaZnO layer and the Si substrate during twice high temperature thermal annealing during growth. Figure 2 shows the room temperature PL of the sample at the surface and 100 nm from substrate, which correspond to Sb-doped ZnO

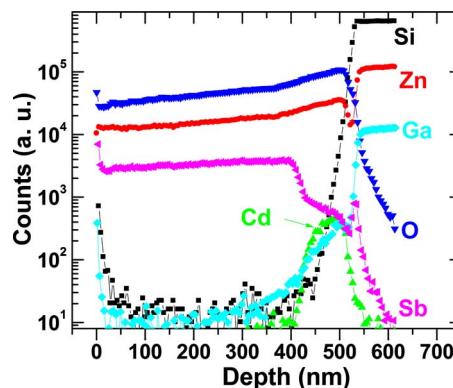


FIG. 1. (Color online) SIMS characteristic of the sample. The interfaces between SbZnO layer and CdZnO layer, CdZnO layer and GaZnO layer can be clearly seen.

^{a)}Author to whom correspondence should be addressed. Electronic mail: jianlin@ee.ucr.edu.

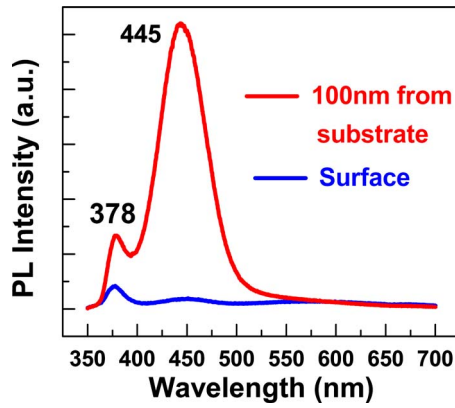


FIG. 2. (Color online) Room temperature PL of the sample from surface (blue line) and 100 nm from substrate (i.e., CdZnO layer) (red line) respectively.

layer and CdZnO layer respectively. PL from Sb-doped ZnO layer (blue line) shows ZnO near band edge (NBE) emission at 378 nm, while PL from CdZnO layer (red line) is dominated by NBE emission of CdZnO active layer at 445 nm. There is also a weaker ZnO NBE emission peak at around 380 nm together with the CdZnO peak, which may come from the GaZnO layer underneath. The PL intensity from CdZnO layer is much stronger than the PL intensity from Sb-doped ZnO layer. This may be due to the lower crystal quality as a result of the incorporation of large Sb atoms into the film.

Figure 3 shows the I - V curve of the sample with voltage configuration shown in the bottom inset. It shows typical diode characteristic under forward bias. Top inset shows good ohmic contact characteristics on both Sb-doped ZnO and Si after RTA. The energy band diagram of the sample is shown in Fig. 4. The room temperature PL peak position is approximately used as the band gap of CdZnO layer, which is about 2.79 eV. The Cd concentration is calculated using the relation $E_g(x) = 3.37 - 2.82x + 0.95x^2$ from Ref. 12 to be 0.22. The electron affinity of CdZnO layer is estimated to be 4.34 eV by assuming it is linearly distributed between 4.3 eV (ZnO) and 4.5 (CdO).^{6,13} So there is a 0.04 eV difference in electron affinity between CdZnO layer and Sb-doped ZnO layer on the top heterointerface, or Ga-doped ZnO layer at the bottom interface, respectively. The electron affinity between Ga-doped ZnO and Si substrate is 0.3 eV.¹⁴ From the

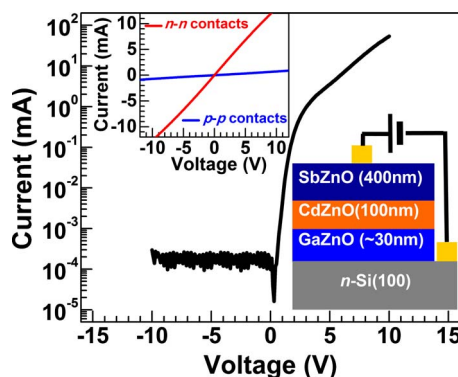


FIG. 3. (Color online) I - V curve of the device, showing rectifying characteristics. Top inset shows the linear I - V of n -contacts (red line) and p -contacts (blue line), respectively. Bottom inset shows device structure of the sample: SbZnO/CdZnO/GaZnO/Si.

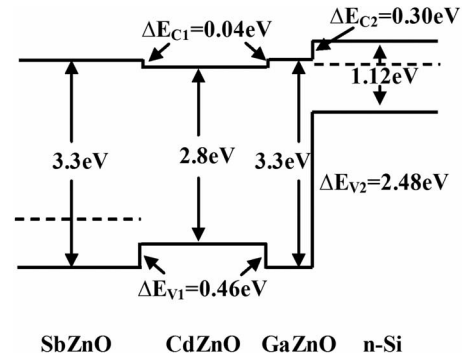


FIG. 4. Band alignment structure of the sample.

band alignment, it is evident that a double heterojunction is formed.

RT EL spectra of the sample at different injection current are shown in Fig. 5. The RT EL emission is dominated by the NBE emission from CdZnO active layer at around 459 nm under 30 mA injection current, which corresponds to the RT PL emission from CdZnO layer. The slight difference in peak positions may come from the non-uniformity of the sample. There are also weak emissions at around 392 nm when injection current goes above 70 mA; it should come from some weak carrier recombinations in Ga-doped ZnO or Sb-doped ZnO layer. Comparing the RT PL and EL, it confirms that the observed EL spectra mainly come from the radiative recombination in CdZnO active layer.

To further confirm the NBE emission from CdZnO, temperature dependent EL measurements from 9 to 300 K were carried out on the sample at an injection current of 80 mA. Figure 6 shows the results. The EL emission peak energy decreases from 2.90 eV (428 nm) at 9 K to 2.63 eV (472 nm) at 300 K. The emission peak at 300 K is slightly different from the one in Fig. 5 (459 nm at 30 mA); it may be due to the nonuniformity of the sample and heat induced band gap shrinkage at higher injection current. The temperature dependence of the exciton energy in direct band-gap material follows Varshni equation, $E(T) = E(0) - \alpha T^2 / (T + \beta)$,^{5,15} α and β are fitting parameters, which are calculated to be $\alpha = 1.2$ eV/K and $\beta = 84$ K. The peak values agree with the fitting curve well. It suggests that the EL emissions come from the NBE emission of CdZnO layer and the red shifts of peak position is due to temperature induced band gap shrinkage.

In summary, ZnO based heterojunction using Sb doped ZnO as p -type layer was grown by MBE. CdZnO active

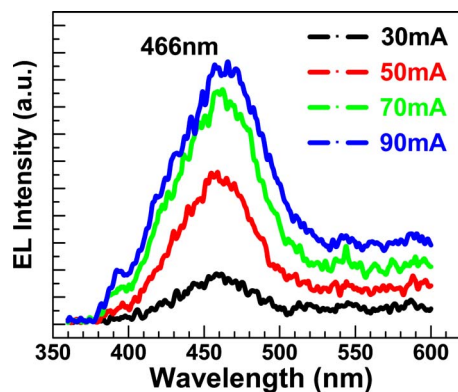


FIG. 5. (Color online) Room temperature EL characteristics of the sample under different injection currents.

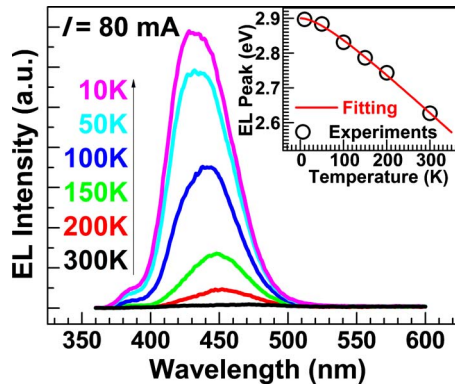


FIG. 6. (Color online) Temperature dependent EL characteristics of the sample under 80 mA injection current, from 10 to 300 K. Inset shows the NBE peak positions as hollow circles against different temperatures and Varshni fitting is shown as a solid line.

layer was used between *p*-layer and *n*-layer to achieve smaller band gap. Dominant blue EL emissions were observed at RT. RT PL measurements at different thicknesses and temperature dependent EL confirmed that these emissions come from the radiative recombinations in CdZnO active layers in the film. Blue emitting LED devices with Sb-ZnO as *p*-type layer are demonstrated.

This work was in part supported by DOE under the Grant No. DE-FG02-08ER46520 and NSF under Grant No. ECCS-0900978.

- ¹D. C. Look, *Mater. Sci. Eng., B* **80**, 383 (2001).
- ²A. Ohtomo, M. Kawasaki, T. Koida, K. Masubuchi, H. Koinuma, Y. Sakurai, Y. Yoshida, T. Yasuda, and Y. Segawa, *Appl. Phys. Lett.* **72**, 2466 (1998).
- ³S. Shigemori, A. Nakamura, J. Ishihara, T. Aoki, and J. Temmyo, *Jpn. J. Appl. Phys., Part 2*. **43**, L1088 (2004).
- ⁴S. Sadofev, S. Blumstengel, J. Cui, J. Puls, S. Rogaschewski, P. Schafer, and F. Henneberger, *Appl. Phys. Lett.* **89**, 201907 (2006).
- ⁵Z. Yang, L. Li, Z. Zuo, and J. L. Liu, *J. Cryst. Growth* **312**, 68 (2009).
- ⁶A. Nakamura, T. Ohashi, K. Yamamoto, J. Ishihara, T. Aoki, J. Temmyo, and H. Gotoh, *Appl. Phys. Lett.* **90**, 093512 (2007).
- ⁷J. W. Mares, M. Falanga, A. V. Thompson, A. Osinsky, J. Q. Xie, B. Hertog, A. Dabiran, P. P. Chow, S. Karpov, and W. V. Schoenfeld, *J. Appl. Phys.* **104**, 093107 (2008).
- ⁸F. X. Xiu, Z. Yang, L. J. Mandalapu, D. T. Zhao, J. L. Liu, and W. P. Beyermann, *Appl. Phys. Lett.* **87**, 152101 (2005); F. X. Xiu, Z. Yang, L. J. Mandalapu, D. T. Zhao, and J. L. Liu, *ibid.* **87**, 252102 (2005).
- ⁹L. J. Mandalapu, Z. Yang, F. X. Xiu, D. T. Zhao, and J. L. Liu, *Appl. Phys. Lett.* **88**, 092103 (2006); L. J. Mandalapu, Z. Yang, S. Chu, and J. L. Liu, *ibid.* **92**, 122101 (2008).
- ¹⁰S. Chu, J. H. Lim, L. J. Mandalapu, Z. Yang, L. Li, and J. L. Liu, *Appl. Phys. Lett.* **92**, 152103 (2008).
- ¹¹J. Y. Kong, S. Chu, M. Olmedo, L. Li, Z. Yang, and J. L. Liu, *Appl. Phys. Lett.* **93**, 132113 (2008).
- ¹²X. J. Wang, I. A. Buyanova, W. M. Chen, M. Izadifard, S. Rawal, D. P. Norton, S. J. Pearton, A. Osinsky, J. W. Dong, and A. Dabiran, *Appl. Phys. Lett.* **89**, 151909 (2006).
- ¹³R. Ferro and J. A. Rodríguez, *Sol. Energy Mater. Sol. Cells* **64**, 363 (2000).
- ¹⁴L. J. Mandalapu, Z. Yang, F. X. Xiu, D. T. Zhao, and J. L. Liu, *Appl. Phys. Lett.* **88**, 112108 (2006).
- ¹⁵Y. P. Varshni, *Physica (Amsterdam)* **34**, 149 (1967).